

Resonance phenomena in the simulation of Calcium ions in a Penning trap using numerical integration methods

Henrik Haug
Axl H Kleven
Live Ljungqvist Storborg
(Dated: September 22, 2025)

The storage of charged particles is a difficult task, and is necessary for several physical sciences including the study of atoms, molecules, anti-particles, and quantum computing [1]. The Penning trap plays a key role in containing and controlling charged particles. Applying the numerical integration methods Forward Euler and Runge-kutta 4 to simulate and study the movement of a single Ca^+ particle in a simple Penning trap with time-independent electric potential, yielded errors on the orders of 10^{-11} to 10^{-7} for RK4, and 10^{-2} to 10^0 for FE, when compared to the analytical solutions for a single particle, using 32'000 time steps over 50 μs . Further, the RK4 integration method was applied to simulate a Penning trap of 100 identical Ca^+ particles without particle-particle interactions with an electric potential influenced by a time-perturbation with varying angular frequency ω_V and amplitude f . Running a simulation over a time $t = 500\mu\text{s}$ with 40'000 time steps, we observed sharp ω_V ranges for storing / ejecting particles. The best combination for storing particles was using $f = 0.1\mu\text{m}$ with $\omega_V = 0\text{MHz} \rightarrow 1\text{MHz}$, as there were 99 - 100 / 100 particles left in this interval. And for and $f = 0.7\mu\text{m}$ with $\omega_V = 1.1\text{MHz} \rightarrow 1.6\text{MHz}$ we observed resonance with 0 / 100 particles left. Running the simulation again for the $f = 0.1\mu\text{m}$ resonance range and applying a fine-grained scan of the ω_V ranges, with particle-particle interactions on, the ω_V ranges remained the same, but the approaching 0.05MHz became transitional with 1-99 remaining particles. As such, our Penning trap allows for using $f = 0.1\mu\text{m}$ with $\omega_V = 1.25\text{MHz}$ for effective storage of particles, and increasing ω_V to 1.4MHz for a highly effective ejection of particles, with an option of a slower ejection using frequencies $\omega_V = 1.3\text{MHz} \rightarrow 1.35\text{MHz}$.

INTRODUCTION

The Penning trap is a commonly used tool in the physical sciences for storing charged particles. The trap is highly useful for long-time storage of particles, and offers a wide range of techniques for manipulating and non-destructively detecting the stored particles. As such, its applications are vast, and it's among other things found: In the physical realization of quantum computers by trapping qubits. At CERN, where the trap is for example used to store and study anti-particles [1].

The trap works by applying a homogeneous magnetic field, and a quadrupole electric field in order to send the charged particles into a periodic orbit. In this periodic orbit there can occur complex resonance phenomena. Studying these resonance phenomena with and without Coulomb effects from particle-particle interactions is the main goal of this article. A good understanding of these resonance phenomena is necessary of important for exactly the applications described above: long term storage, and non-destructive manipulation and detection of the particles. But also for further applications like mass-spectrometry [1].

Our initial model of the penning trap is quite simple, using a constant magnetic and electric potential. This allows for analytical expressions of the equations of motion, angular frequencies, restrictions for bounded solutions, and upper and lower limits of motion. Using these analytical expressions for good comparisons and initial

conditions, our simulation applies the numerical integration techniques Forward Euler and Runge-Kutta 4 to calculate the movement of particles in the trap. The errors and accuracy of these methods are studied by comparing them to the analytical solutions for simple initial conditions. We then use the integration methods to study the resonance phenomena using a time-dependent periodic electric potential. We here study the effects on the storage and resonances of the system by varying the amplitude and frequency of the electric potential. When finding resonance frequencies we will do a fine/grained analysis and find the optimal ranges for storing and ejecting particles.

METHOD & THEORY

Electrodynamics

The electromagnetic equations used in the article are gathered from [2], and are presented here.

From electrodynamics we know that the electric field \vec{E} can be expressed as the gradient of the electric potential \vec{V} (1)

$$\vec{E} = -\nabla\vec{V} \quad (1)$$

We can also describe the electric field at a position \vec{r} created from a set of point charges q_j placed at positions

\vec{r}_j by equation (2).

$$\vec{E}(r) = k_e \sum_{j=1}^n q_j \frac{\vec{r} - \vec{r}_j}{|\vec{r} - \vec{r}_j|^3} \quad (2)$$

Where k_e is the Coulomb constant

$$k_e = 8.987742438 \cdot 10^9 \frac{Nm^2}{C^2}$$

The electric field will, similarly to the magnetic field \vec{B} , create a force on a charged particle q . This force is known as the Lorentz Force (3).

$$\vec{F} = q\vec{E} + q\vec{v} \times \vec{B} \quad (3)$$

Where $\vec{v} = \dot{\vec{r}}$ is the velocity.

For this article we will be applying the electrostatic approximation. Meaning we will ignore the magnetic interactions caused by the magnetic fields created by moving particles. We can safely do this as the particles will be moving far below the speed of light in vacuum, and thus the fields created by motion will be smaller than the Coulomb forces by a factor $O(\frac{v^2}{c^2})$ which is sufficiently small to be ignored.

The Penning trap

The purpose of a Penning trap, as shown in FIG (1), is to contain charged particles. In our case singly charged Calcium ions Ca^+ . It accomplishes this purpose through applying electric fields to trap the particles in the xy-plane (or radial direction). And further utilizing a powerful magnetic field in the z-direction to keep the particles from escaping in the xy-plane, and instead enter orbital motions within the trap.

Our Penning trap will be considered ideal, meaning we can consider the electric field to be described by the electric potential

$$\vec{V}(x, y, z) = \frac{V_0}{2d^2}(2z^2 - x^2 - y^2)$$

Where V_0 is the potential applied to the electrodes. d is defined by

$$d = \sqrt{z_0^2 + \frac{r_0^2}{2}}$$

represents the length scale for the region between the electrodes. z_0 is the distance from the center to one of the end caps (a). While r_0 is the distance from the center to the ring (b).

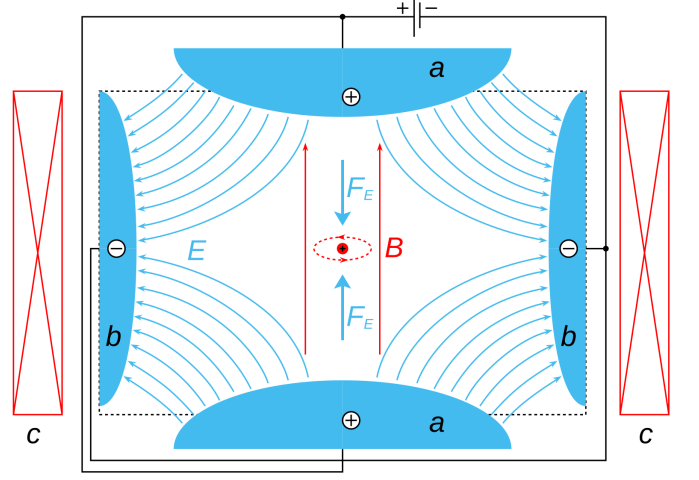


FIG. 1. Schematic illustration of a Penning trap by Arian Kriesch, taken from Wikipedia [3]. The two end caps (a) and a ring (b) are electrodes which set up an electric field. A cylinder magnet (c) sets up a constant, homogeneous magnetic field. The charged particle (red dot) will be confined in the Penning trap by the Lorentz Force caused by the fields. Only the cross section of (b) and (c) are shown.

The applied magnetic field is only in the z-direction, and can thus be described as

$$\vec{B} = B_0 \vec{e}_z = (0, 0, B_0)$$

Where $B_0 > 0$ is the field strength.

Equations of motion

We know Newton's second law as equation (4)

$$\vec{F} = m\vec{a} \quad (4)$$

Where \vec{F} is the sum of forces, m is the mass, and \vec{a} is the acceleration. Using this together with the equation for the Lorentz force (3), we can find expressions for the acceleration in the xyz-coordinates. Using the definitions in equations (5, 6)

$$\omega_0 \equiv \frac{qB_0}{m} \quad (5)$$

$$\omega_z^2 = \frac{2qV_0}{md^2} \quad (6)$$

We find the equations of motion (7, 8, 9). Their derivations are shown in appendix (A).

$$\ddot{x} - \omega_0 \dot{y} - \frac{1}{2} \omega_z^2 x = 0 \quad (7)$$

$$\ddot{y} + \omega_0 \dot{x} - \frac{1}{2} \omega_z^2 y = 0 \quad (8)$$

$$\ddot{z} + \omega_z^2 z = 0 \quad (9)$$

We see that equations (7, 8) are coupled, and are thereby problematic to calculate. We can rewrite these as a single differential complex function using the definition

$$f(t) = x(t) + iy(t)$$

We add the equations together, and describe the new equation using $f(t)$. We get equation (10). See appendix (A) for the derivation.

$$\ddot{f}(t) + i\omega_0 \dot{f}(t) - \frac{1}{2}\omega_z^2 f(t) = 0 \quad (10)$$

The general solution to equation (10) can be written as (11)

$$f(t) = A_+ e^{-i(\omega_+ t + \phi_+)} + A_- e^{-i(\omega_- t + \phi_-)} \quad (11)$$

Where A_{\pm} are positive amplitudes. ϕ_{\pm} are constant phases. Looking at our definition of $f(t)$, we see that our physical coordinates can be found as $x(t) = \text{Re}(f(t))$, $y(t) = \text{Im}(f(t))$. ω_{\pm} is defined as

$$\omega_{\pm} = \frac{\omega_0 \pm \sqrt{\omega_0^2 - 2\omega_z^2}}{2} \quad (12)$$

We want to keep $f(t)$ from blowing up ($|f(t)| < \infty$), as this would cause our particle to fly out of the Penning trap. Remembering Eulers identity

$$e^{i\theta} = \cos \theta + i \sin \theta \quad (13)$$

We see that $f(t)$ will stay a periodic function as long as the exponents are real (or small), and thus not blowing up. This means the expression in the root of equation (12) must stay larger than zero

$$\omega_0^2 - 2\omega_z^2 \geq 0$$

$$\omega_0^2 \geq 2\omega_z^2$$

And thus putting a constraint on our values for ω_0 and ω_z for keeping a bounded solution. From this we can also study the restrictions on our system and particle properties.

$$\begin{aligned} \frac{q^2 B_0^2}{m^2} &\geq 2 \frac{2qV_0}{md^2} \\ \frac{qB_0^2}{m} &\geq 4 \frac{V_0}{d^2} \end{aligned} \quad (14)$$

As long as this difference holds true, our particle will stay in the Penning trap. We can see this by looking at the maximum and minimum values of $f(t)$ in the xy-plane. We can find the upper and lower bounds of $f(t)$ by calculating $|f(t)|^2$, and later taking the square root. For simplicity, We redefine

$$a = \omega_+ t + \phi_+$$

$$b = \omega_- t + \phi_-$$

$$|f(t)|^2 = A_+^2 + A_+ A_- (e^{-ia+ib}) + A_+ A_- (e^{ia-ib}) + A_-^2$$

$$= A_+^2 + A_-^2 + A_+ A_- (e^{i(-a+b)} + e^{i(a-b)})$$

Where we, using eulers identity (13) get

$$= A_+^2 + A_-^2$$

$$+ A_+ A_- (\cos(-a+b) + i \sin(-a+b) + \cos(a-b) + i \sin(a-b))$$

Where we know that

$$\cos(-\theta) = \cos(\theta)$$

$$\sin(-\theta) = -\sin(\theta)$$

Leading to

$$|f(t)|^2 = A_+^2 + A_-^2$$

$$+ A_+ A_- (\cos(a-b) + i \sin(-a+b) + \cos(a-b) - i \sin(-a+b))$$

$$= A_+^2 + A_-^2 + A_+ A_- (2 \cos(a-b))$$

Where the cosine will have a max value of 1, and a min value of -1 leading to

$$f(t)_{\max} = R_+ = \sqrt{A_+^2 + A_-^2 + 2A_+ A_-}$$

$$= \sqrt{(A_+ + A_-)^2}$$

$$= A_+ + A_-$$

$$f(t)_{\min} = R_- = \sqrt{A_+^2 + A_-^2 - 2A_+ A_-}$$

$$= \sqrt{(A_+ - A_-)^2}$$

$$= |A_+ - A_-|$$

Where we have chosen to define the max and min values as R_{\pm} , as they will describe the max and min distances from the origin in the xy-plane.

Specific analytical solutions

For testing our numerical results we will compare them to the results of an analytical solution gathered from [4]. The solution is for a single charged particle q in the Penning trap with the initial conditions

$$\begin{aligned} x(0) &= x_0 & \dot{x}(0) &= 0 \\ y(0) &= 0 & \dot{y}(0) &= 0 \\ z(0) &= z_0 & \dot{z}(0) &= 0 \end{aligned}$$

From equation (9) we thus get the specific solution for movement in the z -direction

$$z(t) = z_0 \cos(\omega_z t) \quad (15)$$

And for movement in the xy -plane we again use $f(t)$ from equation (10), but now using

$$A_+ = \frac{v_0 + \omega_- x_0}{\omega_- - \omega_+} \quad A_- = -\frac{v_0 + \omega_+ x_0}{\omega_- - \omega_+}$$

$$\phi_+ = 0 \quad \phi_- = 0$$

Numbers and units

Our main focus is on very small charged particles. To avoid numerical precision errors when dealing with small numbers we've chosen to use the following set of base units Lists are easy to create:

- Length: micrometre (μm)
- Time: microseconds (μs)
- Mass: atomic mass units (u)
- Charge: the elementary charge (e)

For these base units, we have the following for the Coulomb constant k_e , and the derived SI units for Tesla T and Volt V

$$k_e = 1.38935333 \times 10^5 \frac{u(\mu m)^3}{(\mu s)^2 e^2}$$

$$T = 96.4852558 \frac{u}{(\mu s)e}$$

$$V = 9.64852558 \times 10^7 \frac{u(\mu m)^2}{(\mu s)^2 e}$$

And thus our default Penning trap configuration will have the values

$$B_0 = 1.00T \approx 9.65 \times \frac{u}{(\mu s)e}$$

$$V_0 = 25.0mV \approx 2.41 \times 10^6 \frac{u(\mu m)^2}{(\mu s)^2 e}$$

$$d = 500\mu m$$

With the commonly used ratio

$$\frac{V_0}{d^2} = 9.65 \frac{u}{(\mu s)^2 e}$$

Forward Euler

Forward Euler (FE) is a first-order, single-step numerical integration method. It works for equations on the form

$$\frac{dy}{dt} = f(t, y) \quad (16)$$

where y is an unknown function with a known starting point $y(t_0)$. And $f(t, y)$ is a known function of t and $y(t)$. Using the definition of the derivative on the left hand side we get

$$\frac{y(t+h) - y(t)}{h} + O(h) = f(t, y)$$

Where h is the step size, and $O(h)$ is an error on the order of h . Solving for $y(t+h)$ we get

$$y(t+h) = y(t) + hf(t, y) + O(h^2)$$

Where we can change our notation using

$$y_i = y(t)$$

$$y_{i+1} = y(t+h)$$

$$f(t, y) = f_i$$

And we can make the approximation of leaving out $O(h^2)$ as it is very small. This gives our final equation for the FE method (17)

$$\boxed{y_{i+1} = y_i + hf_i} \quad (17)$$

Application of the Forward Euler method

Our application of the FE method is with the purpose of updating the position of a particle in the penning trap. This particle experiences a sum of forces F , which causes an acceleration a on the particle, following Newtons 2.nd law

$$F = ma = m \frac{d^2 x}{dt^2}$$

Where x is the position of the particle, and dt is the step size. We know the mass m and the force F , and can thus find the acceleration a . Applying the FE method here, we see that we can use

$$a_i = f_i$$

$$v_i = y_i$$

$$dt = h$$

to first update the velocity $v = \frac{dx}{dt}$ for each timestep. Equation (17) becomes (18)

$$\boxed{v_{i+1} = v_i + dta_i} \quad (18)$$

Which we implement numerically to find the updated velocities of the particles. And now knowing the updated velocity, we can update the position x using

$$v_i = f_i$$

$$x_i = y_i$$

Equation (17) now becomes (19)

$$\boxed{x_{i+1} = x_i + dtv_{i+1}} \quad (19)$$

Which we implement numerically to find the updated positions of the particles.

Runge-Kutta 4

Runge-Kutta 4 (RK4) is a fourth-order, single-step numerical integration method. Like FE, it works for equations on the form of equation (16). Being a fourth-order method, RK4 is more accurate than FE, and we can thus use larger step sizes if needed. RK4 consists of a weighted sum of four evaluations as seen in equation (20). This means the method is more computationally expensive than FE, as it requires four evaluations per time step, where two of the evaluations are made at a timestep $t_i + \frac{h}{2}$. Even with this in mind, with a good choice of step size RK4 is generally more efficient and accurate than FE. The derivation of the RK4 method is not shown in this article.

$$\boxed{\begin{aligned} k_1 &= hf(t_i, y_i) \\ k_2 &= hf\left(t_i + \frac{1}{2}h, y_i + \frac{1}{2}k_1\right) \\ k_3 &= hf\left(t_i + \frac{1}{2}h, y_i + \frac{1}{2}k_2\right) \\ k_4 &= hf(t_i + h, y_i + k_3) \\ y_{i+1} &= y_i + \frac{1}{6}(k_1 + 2k_2 + 2k_3 + k_4) \end{aligned}} \quad (20)$$

Application of the Runge-Kutta 4 method

Similarly to our application of the FE method, our application of the RK4 method is with the purpose of updating the position of a particle in the penning trap. And as such our implementation again follows Newtons 2nd law. Following the same order as for FE of first calculating the velocity, and then the position, we run into problems if the method is not implemented in the correct order as the evaluations of k_i for velocity and position will depend on each other. The correct implementation thus goes as seen in equation (21). Where we, when considering particle-particle interactions will have to calculate k_i for all particles before moving onto the next k_{i+1} , as their positions need to be calculated according to the forces between each calculation of k .

$$\boxed{\begin{aligned} k_{x,1} &= dtv_i \\ k_{v,1} &= dta(t_i, x_i, v_i) \\ k_{x,2} &= dt\left(v_i + \frac{1}{2}k_{v,1}\right) \\ k_{v,2} &= dta\left(t_i + \frac{1}{2}h, x_i + \frac{1}{2}k_{x,1}, v_i + \frac{1}{2}k_{v,1}\right) \\ k_{x,3} &= dt\left(v_i + \frac{1}{2}k_{v,2}\right) \\ k_{v,3} &= dta\left(t_i + \frac{1}{2}h, x_i + \frac{1}{2}k_{x,2}, v_i + \frac{1}{2}k_{v,2}\right) \\ k_{x,4} &= dt(v_i + k_{v,3}) \\ k_{v,4} &= dt f(t_i + h, x_i + k_{x,3}, v_i + k_{v,3}) \\ x_{i+1} &= x_i + \frac{1}{6}(k_{x,1} + 2k_{x,2} + 2k_{x,3} + k_{x,4}) \\ v_{i+1} &= v_i + \frac{1}{6}(k_{v,1} + 2k_{v,2} + 2k_{v,3} + k_{v,4}) \end{aligned}} \quad (21)$$

Structure of the simulation

Our simulation is divided into several main branches in order to keep a good and logical structure of the simulation to avoid errors. Their properties can be summarized as follows.

- Particle
 - Stores the following properties of our particle:
 - * Charge q
 - * Mass m
 - * Position \mathbf{r}
 - * Velocity \mathbf{v}
- Penning trap
 - Stores the following properties of our Penning trap:
 - * Magnetic field strength B_0

- * Applied potential V_0
- * Characteristic dimension d
- * All the Particles objects
- Calculates the following:
 - * External electric field \mathbf{E}
 - * External magnetic field \mathbf{B}
 - * Force \mathbf{F} due to the interactions between the particles

Testing the simulation

We have used both the FE and the RK4 methods to evolve our Penning trap system in time. We do this to be able to compare their solutions to each other, as well as later comparing them to the results of the specific analytical solution. Using two particles with the following initial conditions

• Particle 1

- $(x_0, y_0, z_0) = (20, 0, 20) \mu\text{m}$
- $(v_{x,0}, v_{y,0}, v_{z,0}) = (0, 25, 0) \mu\text{m}/\mu\text{s}$

• Particle 2

- $(x_0, y_0, z_0) = (25, 25, 0) \mu\text{m}$
- $(v_{x,0}, v_{y,0}, v_{z,0}) = (0, 40, 5) \mu\text{m}/\mu\text{s}$

These initial values are chosen in order to test that the simulation acts physically according to our expectations for the movements of single particles. Notice that Particle 1 can be used in our analytical solution. Particle 1 has initial positions in the xz-plane and Particle 2 has initial positions in the xy-plane in order to test that the simulation works for all axis. Particle 1 is given an initial velocity only in the y-direction v_y , as we expect this to cause a change of velocity in the x-direction v_x according to the movement in the magnetic field. A velocity v_x would cause a change in v_y , and so we expect the majority of the movement of Particle 1 to be in the xy-plane. Due to the electric fields not being constant, we should also expect a complex periodic motion in the z-direction. Particle 2 however has an initial velocity in the both the y and z-direction v_y, v_z . v_y is expected to cause a similar periodic movement in the xy-plane, although v_z will cause an oscillation in the z-direction due to the electric fields. This movement in the z-direction is thus expected to be more powerful and possibly more complex for Particle 2 than for Particle 1.

We start by comparing FE and RK4 by simulating the:

1. Movement of a single particle (Particle 1) in the Penning trap for a total time $t_{\text{tot}} = 50\mu\text{s}$.
2. Two particles in the Penning trap with and without particle interactions

3. Phase space in the x- and z- planes with and without interactions
4. Trajectories in the xyz-directions for two particles with and without interactions

The purpose of each simulation is:

1. To observe that the particle will be trapped in a cyclical orbit as expected according to our conditions.
2. To observe that the addition of another charged particle cause particle-particle interactions.
3. To continue the testing of the particle-particle interactions, and have a peak at energy conservation.
4. To continue the testing of the particle-particle interactions, and visualising the results to see if they behave physically.

And in order to compare FE and RK4 to the analytical solution, we return to the case of a single particle (Particle 1). We use both FE and RK4 to simulate the movement over $t = 50\mu\text{s}$ using $n = \{4'000, 8'000, 16'000, 32'000\}$ time steps. We use these time steps as they are long enough to give accurate results, but still not too computationally expensive. Using these, we also get to compare the accuracies of our methods, and calculating the error convergence rates require at least three measurements. We compare the results of the integrations to the analytical solutions by looking at their relative error in equation (22), as well as their error convergence rate as seen in equation (23). Estimating the errors is an important part of testing simulations as a low error points to a good simulation. And the error convergence rates tells us how quickly the error decreases as we increase the step size.

$$r_{\text{rel}} = \frac{|\mathbf{r}_{\text{analytical}} - \mathbf{r}_{\text{numerical}}|}{|\mathbf{r}_{\text{analytical}}|} \quad (22)$$

$$r_{\text{err}} = \frac{1}{3} \sum_{k=2}^4 \frac{\log(\Delta_{\text{max}, k} / \Delta_{\text{max}, k-1})}{\log(h_k / h_{k-1})} \quad (23)$$

Where

$$\Delta_{\text{max}, k} = \max_i |\mathbf{r}_{i, \text{exact}} - \mathbf{r}_i|$$

The error convergence rates have different expected values according to which integration method is being used. A first-order method like FE would be expected to have $r_{\text{err}} = 1$, meaning: if you halve the step size, the error will also be halved. And a fourth-order method like RK4 would be to have $r_{\text{err}} = 4$, meaning: if you halve the step size, the error will be halved 4 times, being $\frac{1}{16}$ of the original.

Using the simulation

As we have shortly discussed, we can expect complex periodic motions. This could cause resonance phenomena, which we want to study. We do this by studying the loss of trapped particles as function of the frequency of a time-dependent electromagnetic field. We choose to add a time-dependent perturbation to our applied electric potential V_0 , which thus takes the form of equation (24).

$$V_0 \rightarrow V_1(1 + f \cos(\omega_V t)) \quad (24)$$

Where f is a constant amplitude, and ω_V is the angular frequency of the time-dependent potential term.

We fill our penning trap with 100 randomly initialized particles, and run simulations using $t = 500\mu s$ with amplitudes $f = \{0.1, 0.4, 0.7\}\mu m$ and a frequency in the range $\omega_V \in (0.2, 2.5) MHz$. We wish to study:

1. The amount of particles left in the trap with particle-particle interactions turned off.
2. The effect of particle-particle interactions on the resonances of the system.

Studying 1) will simply be done by looking at the amount of particles still left as a function of ω_V for the three different f . Studying 2) will be done by performing fine-grained frequency scans around our uncovered resonances, and study the effect of having particle-particle interactions on or off. We will also repeat 1) with particle-particle interactions on.

These cases are important to study because:

1. This will help us understand how the Penning trap works in practice, and how the particles respond to different frequencies. This could allow us to understand how to use the Penning trap for both trapping particles, and pushing them out when needed using the frequencies and amplitudes.
2. This will further help us understand how the Penning trap works in practice, and allow us to get an idea of how significant the particle-particle interactions are in the Penning trap when trying to keep the particles trapped / push them out.

We do this by defining the \mathbf{E} and \mathbf{B} fields outside the trap to be zero, as a particle that escapes the trap will now simply 'fly away', and it essentially won't interact with the trapped particles (\vec{r} goes to infinity). Finally we count the remaining particles after the simulation.

Tools

For our code we have used github, and our code can be found here [5]. Our code is mainly written in C++ where

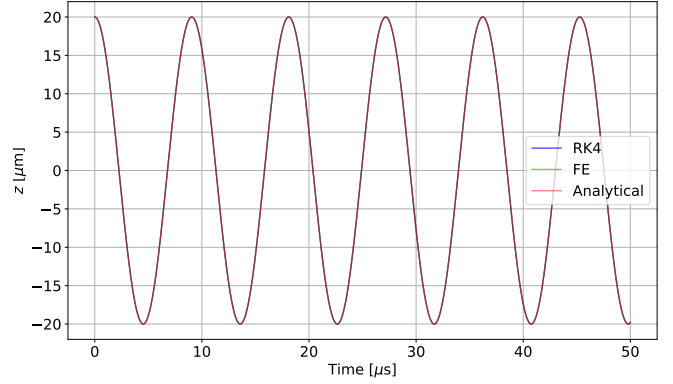


FIG. 2. The motion of particle 1 in the z -direction over $50\mu s$ using 32'000 time steps using the analytical solution, and the integration methods RK4 and FE.

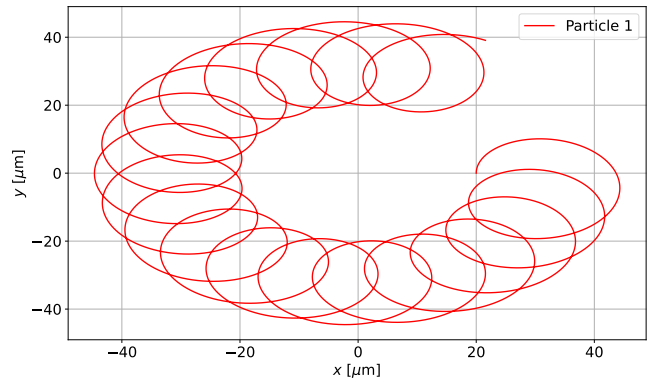


FIG. 3. The motion particle 1 in the xy -plane over $50\mu s$ using 32'000 time steps using the analytical solution.

we have used the additional Armadillo [6] library. For creating figures we have used Python, with the following libraries: matplotlib [7], and numpy [8].

RESULTS & DISCUSSION

Testing the simulation

The movement of particle 1 in the penning trap for a total time of $50\mu s$ using 32'000 time steps is shown in FIG (2) for the z -direction, and in FIG (3) for xy -plane. The movement of both particles is shown in FIGs (3, 5, 6) for the xy -plane with and without particle interactions. We remember that our analytical solution only works for particle 1, and as such the movements of two particles will only be for FE and RK4. From the figures previously mentioned we can see that the FE and RK4 integration methods agree very well with the analytical solution for the movement particle 1 in the penning trap in the xyz -directions. The particles clearly enter complex periodic motions which appear to trap the particle

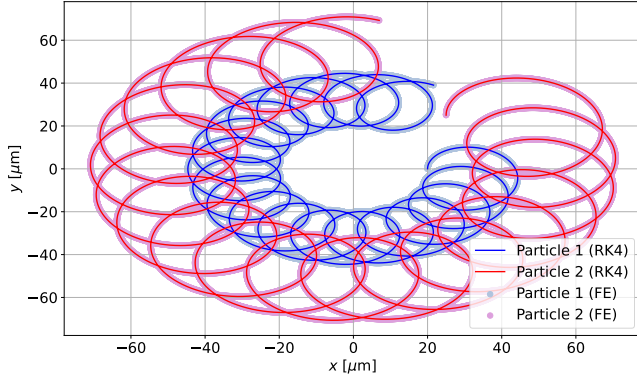


FIG. 4. The motion of particle 1 and particle 2 without particle interactions in the xy-plane over $50\mu s$ using 32'000 time steps using the integration methods RK4 and FE.

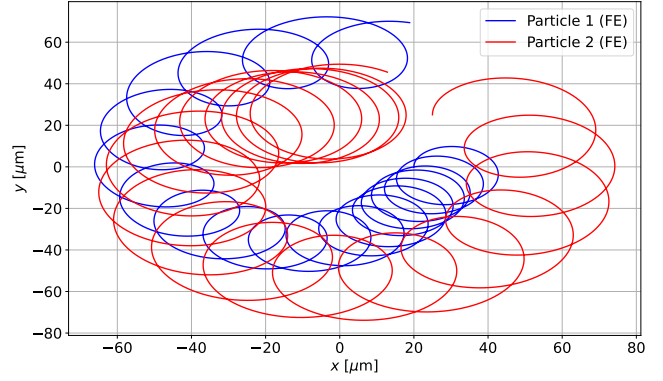


FIG. 6. The motion of particle 1 and particle 2 with particle interactions in the xy-plane over $50\mu s$ using 32'000 time steps using the integration method FE.

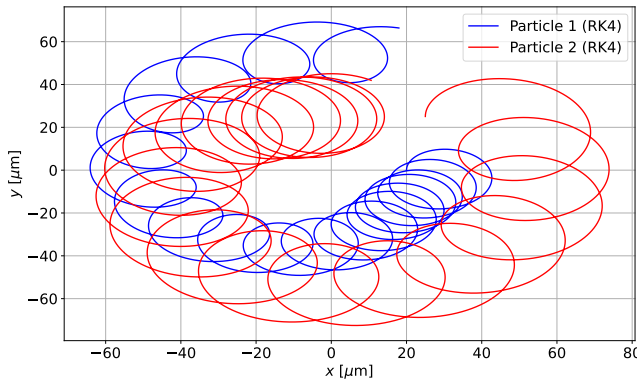


FIG. 5. The motion of particle 1 and particle 2 with particle interactions in the xy-plane over $50\mu s$ using 32'000 time steps using the integration method RK4.

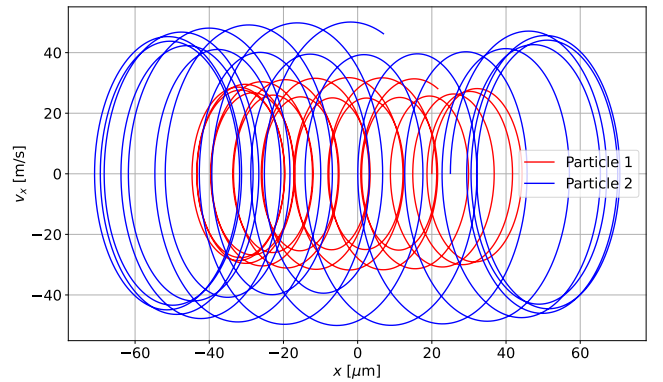


FIG. 7. Phase space in x-direction of particle 1 and particle 2 without particle interactions over $50\mu s$ using 32'000 time steps per simulation, using the integration method RK4.

for an indefinite time, for all cases. For the analytical case, this is expected, as our values for ω_z given the initial values of particle 1 fulfill our requirement in equation (14). Further, we can tell that the complex periodic motions the particles enter when using the integration methods clearly resemble the motion of the analytical solution, and are very very similar for particle 1 without particle interactions. As such, the integration methods produce results that appear correct and physical. When adding interactions, we can clearly see that the particles 'push' on each other, but still enter complex periodic motions, staying in the trap. Here, FE and RK4 even seem to agree very well on the trajectories, which is surprising, as the system is expected to show chaotic properties when adding particle-particle interactions, and as such, even just a small cumulative error difference between the methods should cause vastly different movements. This points to both the methods being accurate.

The phase-space in the x- and z-planes are shown in FIGs (7, 8, 9, 10) with and without particle interactions.

These previously mentioned figures of the phase-space are as expected, as we in the z-space without particle

interactions expect perfect circles. We can see this from FIG (2) where we have what appears to be a cosine wave, which is made using a perfect circle. For the x-space we also expect something similar to circles, but 'moving' back and forth in a periodic motion. This is also visible in FIG (3) where the velocity in the x-direction has its absolute maximum at the top and bottom of a near-circle, and its minima (0) at the sides of the same near-circle, and this near-circle moves in circles itself (causing the 'moving' back and forth). When adding particle-particle interactions we still expect periodic motions (circles in phase space), but we expect them to appear more chaotic and opposing in motion as the particles push on each other. This is what we observe in the figures, and as such the integration methods appear to agree very well with the analytical solutions, and they appear to behave physically.

Trajectories in the xyz-directions for two particles are shown in FIGs (11, 11) with and without particle interactions. We can here clearly tell that the particles follow complex periodic motions, and the addition of particle interactions cause the particles to push each other away as

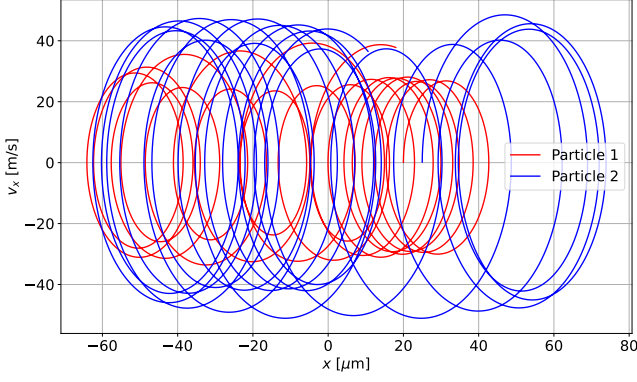


FIG. 8. Phase space in x-direction of particle 1 and particle 2 with particle interactions over $50\mu s$ using 32'000 time steps per simulation, using the integration method RK4.

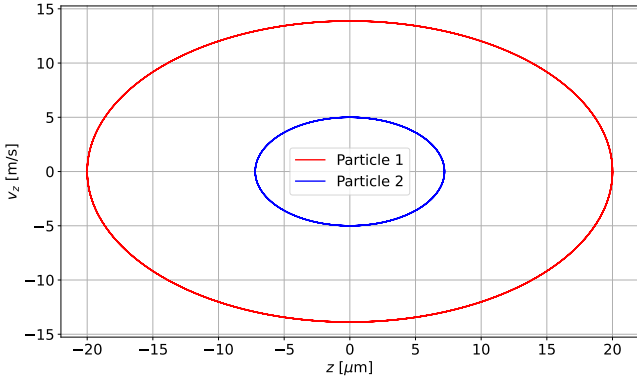


FIG. 9. Phase space in z-direction of particle 1 and particle 2 without particle interactions over $50\mu s$ using 32'000 time steps per simulation, using the integration method RK4.

expected, but still enter complex periodic motions. This follows expectations and appears physical.

The relative error between the simulations and the analytical solutions for the movement in the x-direction for the four different time steps is shown in FIG (13). And the error convergence rates for the integration methods using the four time steps becomes

$$r_{\text{err, FE}} = 1.39675$$

$$r_{\text{err, RK4}} = 4$$

From the previous figures of the analytical and numerical solutions, we can see that the numerical methods agree very well with analytical. Although there is no visible error, we should still expect an increasing error over time. And we expect an increase in time steps to decrease the error. For both methods this is clearly the case, and errors are also of a fitting order when compared to the visualizations (way smaller than 1). This means our implementation of the methods appear correct, and that using RK4 with a small time step is the most accurate.

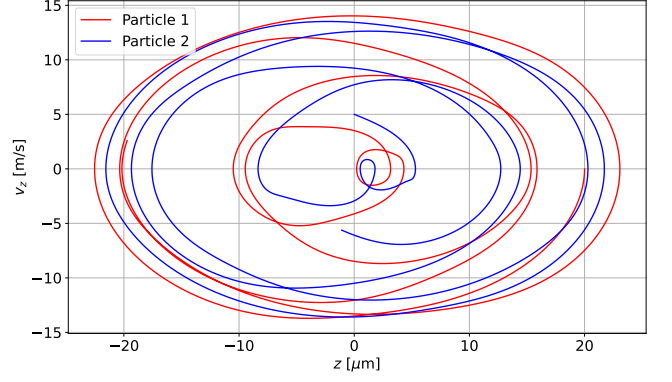


FIG. 10. Phase space in z-direction of particle 1 and particle 2 with particle interactions over $50\mu s$ using 32'000 time steps using the integration method RK4.

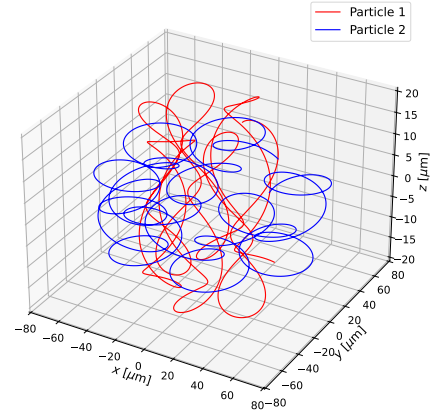


FIG. 11. Motion of particle 1 and particle 2 in the xyz-directions without particle interactions over $50\mu s$ using 32'000 time steps using the integration method RK4.

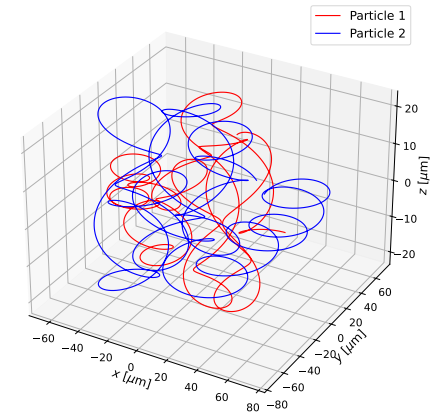


FIG. 12. Motion of particle 1 and particle 2 in the xyz-directions with particle interactions over $50\mu s$ using 32'000 time steps using the integration method RK4.

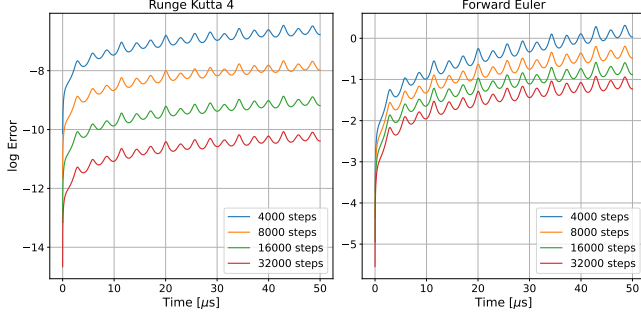


FIG. 13. Relative error of the four different time steps of the integration methods FE and RK4 against the analytical solution for the motion of particle 1 in the xyz-directions over $50\mu s$ using four different time steps as shown in the figure.

The oscillatory behavior of the errors could possibly be explained by the fact that neither RK4 and FE are energy conserving integration methods, and as such their energies (and thus calculated values) can drift and oscillate from and around the true values.

We expected the error convergence rate for FE to be equal to 1, but using such a small sample size the result is within expectation. For RK4, we expected a value of 4, and as such our calculated value is clearly correct. The calculation of error rate is heavily related to the relative error, and a larger error convergence rate should result in a larger distance between the relative errors when changing the time steps. This is clearly visible in FIG (13). In this figure, we also see that the error is on scales of $10^{-11} \rightarrow 10^{-7}$ for RK4 and $10^{-2} \rightarrow 10^0$ for FE. As such it is not surprising that the results turns out correct when the error is this small. From this we can yet again conclude that the methods appear correctly implemented, with RK4 with a small time step being the most accurate.

Using the simulation

Filling our penning trap with 100 randomly initialized particles, and running simulations with RK4 over $t = 500\mu s$, with 40'000 time steps, for three different amplitudes $f = \{0.1, 0.4, 0.7\}\mu m$ and a frequency in the range $\omega_V \in (0.2, 2.5) MHz$ (increasing with $0.02 MHz$ per step) without particle-particle interactions¹. We get FIGs (14, 15, 16) showing how many particles are left for a given amplitude as a function of frequency. We can clearly see that we have resonance frequencies causing particles to escape, as all the particles either escape or stay in the trap for the different frequencies. The frequencies that help the particles escape the trap (positive

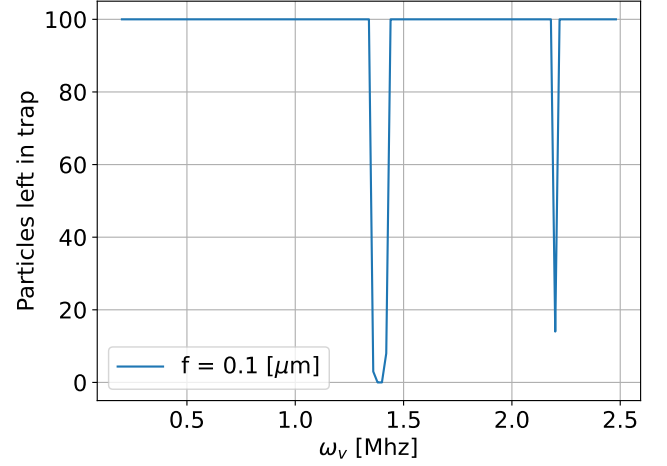


FIG. 14. Amount of particles left in the trap as a function of frequency of the applied \mathbf{E} field (ω_V) after simulating 100 randomly initialized particles over $500\mu s$ with an amplitude $f = 0.1\mu m$ for each frequency, using RK4.

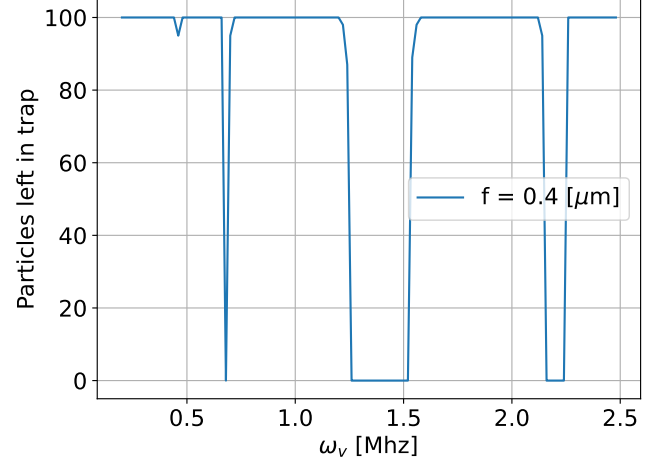


FIG. 15. Amount of particles left in the trap as a function of frequency of the applied \mathbf{E} field (ω_V) after simulating 100 randomly initialized particles over $500\mu s$ with an amplitude $f = 0.4\mu m$ for each frequency, using RK4.

resonance), do so as they align with the complex periodic motions of the particles, and thus increase their energies until they are able to escape. The frequencies that cause a lot of particles to stay in the trap (negative resonance), is also a case of the same frequency phenomena with opposite results; the applied frequency opposes the complex periodic motions of the particles, and their energies don't increase. We see that an increase in amplitude f will increase the range of positive resonance frequencies. This means that a larger frequency of $f = 0.7\mu m$ at frequencies between $1.2 MHz$ and $1.6 MHz$ is the best for sending out particles, while a smaller amplitude at frequencies around $1 MHz$ will keep the particles trapped.

We thus choose to perform the fine-grained scans with

¹ We switch off particle-particle interactions as they would be very computationally expensive for 100 particles

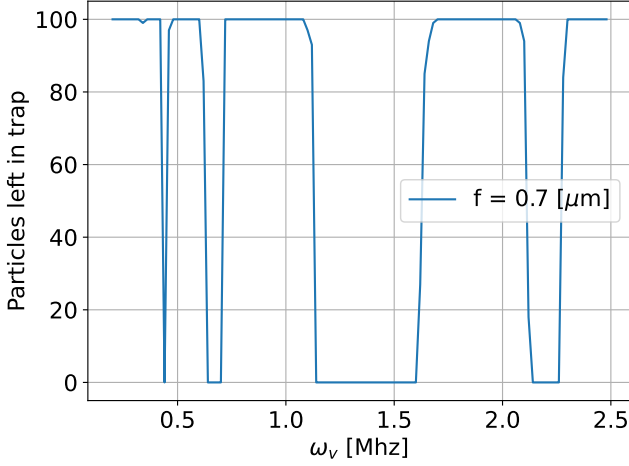


FIG. 16. Amount of particles left in the trap as a function of frequency of the applied \mathbf{E} field (ω_V) after simulating 100 randomly initialized particles over $500\mu s$ with an amplitude $f = 0.7\mu m$ for each frequency, using RK4.

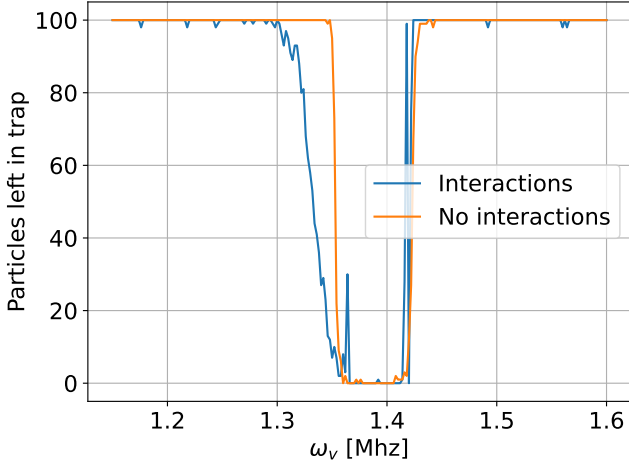


FIG. 17. Fine-grained frequency scan without particle-particle interactions around resonance frequency $f = 0.1\mu m$, $\omega_V = 1.15 \rightarrow 1.6 MHz$ found in FIG (16).

particle-particle interactions turned on around the positive resonance area for $f = 0.1\mu m$ and frequency $\omega_V = 1.15 \rightarrow 1.6 MHz$ (increasing $0.002 MHz$ each step). The amount of particles left in the trap as a function of the fine-grained frequency is shown in FIG (17). We see that the particle-particle interactions cause the steep drop in the figure without particle-particle interactions to turn more gradual coming from the lower frequencies, but still remaining fairly steep for the higher frequencies.

This result enables us to control how we store and eject the particles from the trap. If we wish to store the particles for a long time, we could use $f = 0.1\mu m$ with $\omega_V = 1.2 MHz$. And if we wish to send them out really fast, we could increase the frequency to about

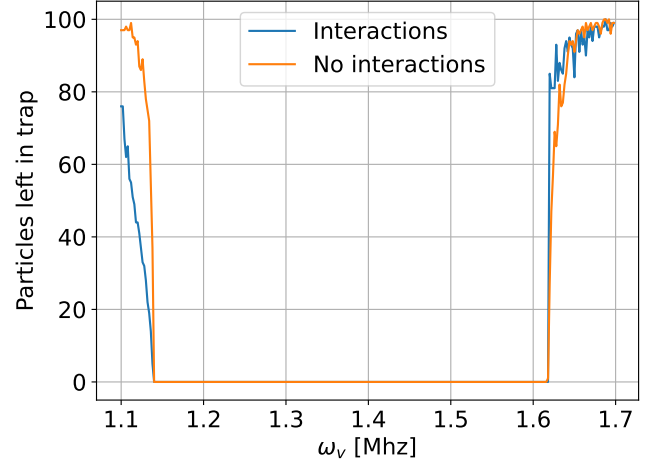


FIG. 18. Same as FIG (17), but for $f = 0.7\mu m$, $\omega_V = 1.1 MHz \rightarrow 1.7 MHz$ using $0.002 MHz$ per step.

$\omega_V = 1.4 MHz$. Or, if we wanted to send them out over a longer range of time, we could use a frequency of $\omega_V = 1.3 MHz \rightarrow 1.35 MHz$. This result also has the advantage that we only need to change the frequency to control the particles, instead of having to change the frequency and amplitude at the same time.

In FIG (17) we see that there are slight irregularities within the resonance frequency range. We wish to study if this is the case for the positive resonance frequencies for $f = 0.7\mu m$ as well. We re-run the fine-grained analysis with $f = 0.7\mu m$ for $\omega = 1.1 MHz \rightarrow 1.7 MHz$, increasing with $0.002 MHz$ per step, and get FIG (18). We observe no irregularities within this resonance frequency, and as such, using $f = 0.7\mu m$ with $\omega = 1.1 MHz \rightarrow 1.7 MHz$ appears to be the most stable resonance frequency for ejecting particles.

Further research on the Penning Trap is needed for an even better understanding of such an important scientific tool. We observe that when the particle-particle interactions are added in FIG (17), there is still a chance for 1 particle to escape the trap. Could this potentially be avoided by using a time-perturbation in the magnetic field as well? Or could the shape of the penning trap play a role? We know that the particles move in circular motions, and as such, could a circular trap be more efficient? And what would happen for cases of particles with different masses? This last question would be the most intriguing to answer if we had more time, as it could enable us to store a larger variety of particles.

CONCLUSION

We have applied the numerical integration methods Forward Euler and Runge-kutta 4 for the simulation of the movement of Ca^+ particles in a simple Penning Trap. When using a simple particle over $50\mu s$ with 32'000 time

steps, with a time-independent electric potential we observed results appearing physical, with errors for both methods on the orders of 10^{-11} to 10^{-7} for RK4, and 10^{-2} to 10^0 for FE. Further applying the RK4 integration method we simulated 100 particles with and without particle interactions in a Penning trap influenced by a time-dependent perturbation with varying angular frequency ω_V and amplitude f . Using $t = 500\mu s$ and a varying time step, we observed clear amplitude and frequency combinations for storing and ejecting particles. When ignoring particle-particle interactions, the best combination for storing particles was using $f = 0.1\mu m$ with

$\omega_V = 0MHz \rightarrow 1MHz$, as there were 99 - 100 / 100 particles left in this interval. And for and $f = 0.7\mu m$ with $\omega_V = 1.1MHz \rightarrow 1.6MHz$ we observed resonance with 0 / 100 particles left. When adding particle-particle interactions for the $f = 0.1\mu m$ resonance range, the frequency ranges remained the same, but the approaching $0.05MHz$ became transitional with 1-99 remaining particles. As such, our Penning trap allows for using $f = 0.1\mu m$ with $\omega_V = 1.25MHz$ for effective storage of particles, and increasing ω_V to $1.4MHz$ for a highly effective ejection of particles, with an option of a slower ejection using frequencies $\omega_V = 1.3MHz \rightarrow 1.35MHz$.

-
- [1] Wikipedia, [Penning trap](#).
 - [2] A. Kvellestad, [Reminder on electrodynamics and classical mechanics](#) ().
 - [3] A. Kriesch, [File:penning trap.svg](#).
 - [4] A. Kvellestad, [Specific analytical solution](#) ().
 - [5] L. L. S. Henrik Haug, Axl H Kleven, [Project 3](#).
 - [6] R. C. Conrad Sanderson, Armadillo: a template-based c++ library for linear algebra., Journal of Open Source Software **1**, 7 (2016).
 - [7] J. D. Hunter, Matplotlib: A 2d graphics environment, [Computing in Science & Engineering](#) **9**, 90 (2007).
 - [8] C. R. Harris, K. J. Millman, S. J. van der Walt, R. Gommers, P. Virtanen, D. Cournapeau, E. Wieser, J. Taylor, S. Berg, N. J. Smith, R. Kern, M. Picus, S. Hoyer, M. H. van Kerkwijk, M. Brett, A. Haldane, J. F. del Río, M. Wiebe, P. Peterson, P. Gérard-Marchant, K. Sheppard, T. Reddy, W. Weckesser, H. Abbasi, C. Gohlke, and T. E. Oliphant, Array programming with NumPy, [Nature](#) **585**, 357 (2020).

Appendix A: Equations of motion

For all xyz, we will start by combining Newtons second law (4) and the Lorentz force (3) in the sum of forces from newtons second law.

$$\vec{F} = m\vec{a} = q\vec{E} + q\vec{v} \times \vec{B}$$

Where we use our electric potential \vec{V} and magnetic field \vec{B} from the Penning trap.

For x we have:

$$F = m\ddot{x} = q\frac{V_0}{2d^2}\left(-\frac{\delta\vec{V}}{\delta x}\right) + q(\vec{x} \times B_0\vec{e}_z)$$

Where we use the right hand rule to see that $\hat{x} \times \hat{z} = \hat{y}$, and so we get

$$\ddot{x} = \frac{qV_0}{2md^2}x + \frac{q\dot{y}B_0}{m}$$

And we use our definitions from equations (5, 6) giving

$$\ddot{x} - \omega_0\dot{y} - \frac{1}{2}\omega_z^2x = 0$$

Now moving on to y:

$$F = m\ddot{y} = q\frac{V_0}{2d^2}\left(-\frac{\delta\vec{V}}{\delta y}\right) + q(\vec{y} \times B_0\vec{e}_z)$$

Where we use the right hand rule to see that $\hat{y} \times \hat{z} = -\hat{x}$, and so we get

$$\ddot{y} = \frac{qV_0}{2md^2}x + \frac{q(-\dot{x})B_0}{m}$$

And we use our definitions from equations (5, 6) giving

$$\ddot{y} + \omega_0\dot{x} - \frac{1}{2}\omega_z^2y = 0$$

Now moving on to z:

$$F = m\ddot{z} = q\frac{V_0}{2d^2}\left(-\frac{\delta\vec{V}}{\delta z}\right) + q(\vec{z} \times B_0\vec{e}_z)$$

Where we know that $\hat{z} \times \hat{z} = 0$, and so we get

$$\ddot{z} = \frac{qV_0}{2md^2}z + 0$$

And we use our definition from equation (6) giving

$$\ddot{z} + \omega_z^2z = 0$$

Further, for defining our new function using our complex function $f(t)$ we sum up equations (7, 8) as follows:

$$\ddot{x} - \omega_0\dot{y} - \frac{1}{2}\omega_z^2x + i(\ddot{y} + \omega_0\dot{x} - \frac{1}{2}\omega_z^2y) = 0$$

$$\ddot{x} + i\ddot{y} + \omega_0(i\dot{x} - \dot{y}) - \frac{1}{2}\omega_z^2(x + iy) = 0$$

$$\ddot{x} + i\ddot{y} + i\omega_0(\dot{x} + i\dot{y}) - \frac{1}{2}\omega_z^2(x + iy) = 0$$

$$\ddot{f}(t) + i\omega_0\dot{f}(t) - \frac{1}{2}\omega_z^2f(t) = 0$$